

Optical properties of bismuth oxide thin films prepared by reactive magnetron sputtering

L. LEONTIE*

Faculty of Physics, "Al. I. Cuza" University, 11 Carol I Boulevard, R-700506 Iasi, Romania

The optical properties, absorption in the domain 2.50-4.30 eV and the optical functions, n , k , ε_1 , and ε_2 , in the range 1.24-6.50 eV, for bismuth oxide films prepared by reactive magnetron sputtering, onto glass and amorphous quartz, at room temperature, have been investigated. Sputtered films ($d=0.05$ - $1.80 \mu\text{m}$) are preponderantly amorphous, also containing Bi_2O_3 nanocrystallites, in incipient phase. From optical absorption data the optical band gaps of investigated sputtered films have been determined: $E_{\text{ga}}=2.68$ - 2.73 eV (amorphous phase) and $E_{\text{go}}=3.55$ eV (optical direct gap). By studying the dispersion of optical functions, a series of particularities at 3.60 eV, 4.30 eV, 4.80 eV, 5.55 eV, and 6.20 eV are evidenced for sputtered films; they correspond to direct band-to-band transitions in the nanocrystalline Bi_2O_3 .

(Received February 2, 2005; accepted May 18, 2006)

Keywords: Bismuth oxide, Amorphous thin films, Ellipsometry, UV-VIS absorption, Spectroscopy, Reflection spectroscopy

1. Introduction

Bismuth oxide is a representative oxidic semiconducting material, with various physical and chemical properties determined by its numerous modifications [1,2]. In form of thin films, it possesses significant values of band gap, refractive index and dielectric permittivity. Besides, it shows remarkable (UV) photosensitivity and photoluminescence [3-7].

The physical properties of bismuth oxide thin films are strongly dependent on the preparation technology, which moulds the phase composition of the samples; thus, the optical gap, E_{go} , is seen to vary from about 2 eV, to 3.96 eV [2-4,7-10].

The peculiar characteristics of bismuth oxide recommend it for a wide range of applications in the solid-state technology: from optical coatings [11], to optoelectronics [12] and ceramic glass manufacturing [13-18].

A series of technological applications of bismuth oxide thin films uses its photocatalytic properties and the caption of polar gases in the gas sensors [19, 20]. They are based on the spectrum of surface states that can be determined, in the case of submicron films, by analyzing the dispersion of optical constants in the domain of fundamental absorption band.

The study of optical properties of bismuth oxide thin films, which is of great experimental and theoretical interest, have been reported by a number of authors [2-4, 8,9,12,21-27].

In this paper we investigate the optical properties of bismuth oxide films prepared by reactive magnetron sputtering.

2. Experimental

Bismuth oxide films were deposited by magnetron reactive sputtering onto glass and amorphous quartz at

temperature of about 300 K, at a chamber pressure $p = 4$ mTorr, using Bi_2O_3 (000) pellets, in an atmosphere $\text{Ar}:\text{O}_2$ (9:1). The thickness of respective films, determined by a TENCOR P-2 Long Scan profilometer, ranged between 0.05 and 1.80 μm .

The crystalline structure and growth dynamics were investigated by means of XRD ($\text{Cu K}\alpha$ radiation) and AFM techniques. As revealed by X-rays diffraction analyses, the use of sputtering method resulted in films with mixed structure, amorphous (preponderante) and crystalline, the last one consisting of nanocrystallites of Bi_2O_3 .

In the study of transmission and reflection spectra in the range 2.50-6.50 eV, a SPECORD M40 spectrophotometer was used, equipped with a device for reflectance measurements at small incidence angles, $\theta \leq 8^\circ$.

In the region of the fundamental absorption threshold, the dispersion of optical constants, n and k (the refraction index and the extinction coefficient, respectively), was determined by means of the ellipsometric method (a VASE ellipsometer was used).

3. Results and discussion

3.1. Basic equations

In the region of fundamental absorption edge, the absorption coefficient, α , of a plan-parallel sample with thickness d , can be calculated by using the equation [28]:

$$T = \frac{(1-R)^2 + 4R \sin^2 \psi}{e^{-\alpha d} (1-R^2) - 2R \cos 2(\delta + \psi)}, \quad (1)$$

where T and R denote the transmission and reflection factors, respectively, and quantities δ and ψ are given by

$$\delta = \frac{4\pi nd}{\lambda} \text{ and } \psi = \frac{\arctan 2k}{n^2 + k^2 + 1}, \quad (2)$$

n denoting the refraction index.

In the region within fundamental absorption band, the optical constants of the material, n and k , were calculated from $R(h\omega)$ spectra ($h\omega$ is the photon energy), registered at normal incidence, by means of equations [29]:

$$n = \frac{1 - R}{1 + R - 2\sqrt{R} \cos \Delta}, \quad (3)$$

$$k = \frac{2\sqrt{R} \sin \Delta}{1 + R - 2\sqrt{R} \cos \Delta}. \quad (4)$$

In the above expressions, Δ is the phase angle considered at frequency ω_0 , which is determined by Kramers-Kronig equation [29]:

$$\Delta_{\omega_0} = -\frac{\omega_0}{\pi} \int_0^{\infty} \frac{\ln R}{\omega^2 - \omega_0^2} d\omega. \quad (5)$$

3.2. Optical absorption in the vicinity of fundamental absorption edge

In Fig. 1 typical absorption spectra for sputtered micron bismuth oxide films are presented. As can be easily observed, the dependence $\alpha(h\omega)$ shows two distinct portions, separated at $h\omega \sim 3$ eV.

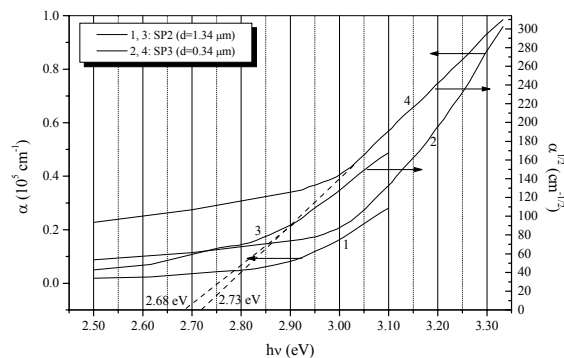


Fig. 1. Typical absorption spectra of sputtered films.

For photon energies $h\omega \leq 3$ eV, the absorption coefficient is slowly decreasing at increasing wavelengths, irrespective of film thickness (between 0.05 and 1.50 μm). This behavior can be generally explained by phonon scattering on structural defects-in the present case, on

granules of micrometric dimensions, which are characteristic to film structure (Fig. 2).

In the spectral domain $h\omega \geq 3$ eV, the absorption coefficient increases at increasing photon energies. This rise is well fitted by a power law with an exponent equal to 1/2. Linear dependences of $\alpha^{1/2} = f(h\omega)$ can be observed in both amorphous films and for indirect transitions in crystalline films [27, 28, 30]. The XRD examination shows only weak lines characteristic to Bi_2O_3 . Taking into account the above results, as well the relatively slow increase of α (less than 5 times, when the photon energy is increased from 3 eV to ~ 3.35 eV), we can state that the sputtered films are characterized by a preponderant amorphous phase, which also contains crystallization germs of bismuth oxide, in incipient phase.

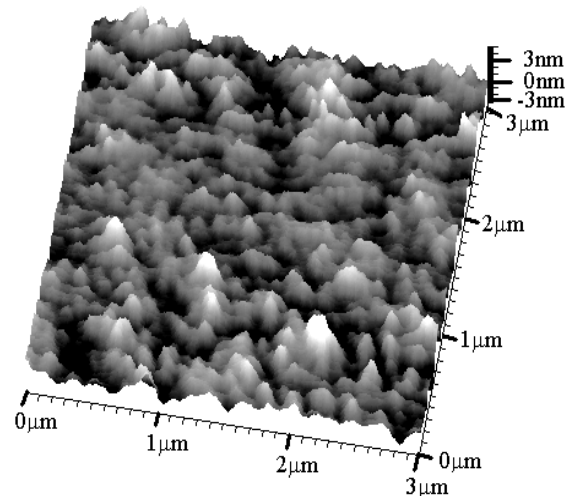


Fig. 2. AFM image of a sputtered film: sample SP4 ($d=0.07 \mu\text{m}$).

The width of optical gap, E_{ga} , for respective (amorphous) films, lies between 2.68 eV and 2.73 eV (Fig. 1). The band gap of amorphous bismuth oxide films is about 0.1 eV smaller than E_{go} value of monocrystalline Bi_2O_3 at the same temperature [4, 24]. The mentioned decrease can be explained by the presence of band tails for the conduction and valence bands, which show an exponential decrease of the density of states (DOS) within the forbidden band [31].

For sputtered bismuth oxide films, at energies corresponding to the depth of the absorption band, the absorption spectrum evidences a very marked increase (Fig. 3): in an energy range of only 0.07 eV, beginning to 3.52 eV, the absorption coefficient increases more than 4 times. Since short-distance order, characteristic to nanocrystalline phase of bismuth oxide, maintains in the case of amorphous films, the threshold by 3.52 eV has to be interpreted as electron interband transition corresponding to an optical gap of 3.55 eV (Fig. 3).

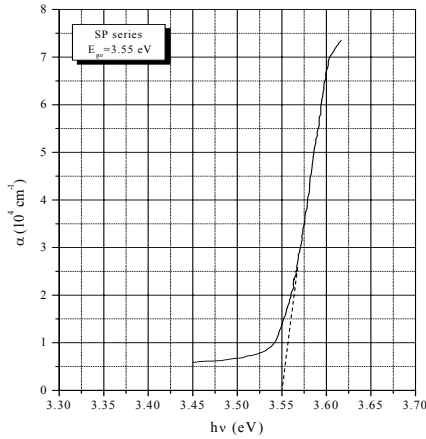


Fig. 3. Optical absorption of films from SP series.

3.3. Dispersion of optical constants

Fig. 4 presents the dependences $n(\hbar\omega)$ and $k(\hbar\omega)$ in the case of sputtered bismuth oxide films, calculated from reflectance spectra, on the basis of equations (3) and (4). The film thickness varies from 0.07 to $\sim 1.80 \mu\text{m}$. As can be ascertained from mentioned figure, the refraction index, n (curves 1, 2, and 3), tends to decrease at increasing photon energies in the range $\hbar\omega > 3.20 \text{ eV}$, irrespective of sample thickness, while the extinction coefficient, k (curves 4, 5 and 6), shows a similar behavior for energies above $\sim 3.60 \text{ eV}$.

As was demonstrated by studying the spectral dependence of α in the domain $\sim 3.20\text{--}3.50 \text{ eV}$, for submicron films deposited onto quartz and sapphire, the absorption quite slowly increase with photon energy. The mentioned saturation of absorbance can be explained by the particularities of the spectrum of energy bands in the case of bismuth oxide. The slow decrease of n and k at increasing photon energies, corresponding to the depth of fundamental absorption band, can be explained by a decrease of DOS in the electronic bands, in different high symmetry points of Brillouin zone, as well as by a high density of surface states for as-prepared films.

On the decreasing part of the spectral curve for the extinction coefficient, k (Fig. 4), one evidence four particularities in form of thresholds localized in the range $3.50\text{--}6.20 \text{ eV}$. In the case of thinnest films (curve 4), three particularities, A ($\hbar\omega=4.30 \text{ eV}$), B ($\hbar\omega=4.85 \text{ eV}$), and A* ($\hbar\omega=3.55 \text{ eV}$), are evidenced, while supplementary higher energy maximums, C ($\hbar\omega=5.50 \text{ eV}$) and D ($\hbar\omega=6.20 \text{ eV}$), are characteristic to films with larger thickness (curve 5). At increased film thickness, the structure of $k(\hbar\omega)$ spectrum simplifies, so that for films of about $1.80 \mu\text{m}$ thick two particularities are shown: a broad maximum at 3.60 eV and a threshold localized at $\sim 5.55 \text{ eV}$ (curve 6).

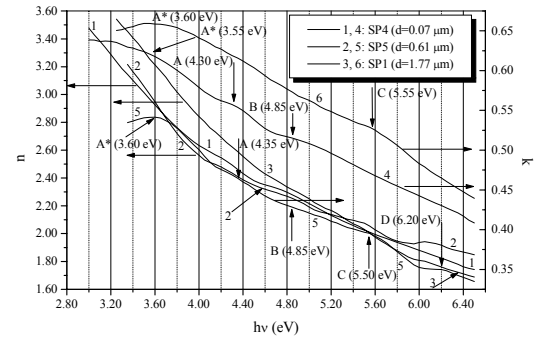


Fig. 4. Dispersion of optical constants, $n(\hbar\omega)$ and $k(\hbar\omega)$ for as-prepared films.

Highly relevant informations concerning the structure of electron energy bands and DOS in semiconducting and dielectric materials can be obtained by analyzing the dispersion of dielectric function, $\varepsilon(\hbar\omega)$. In the domain of fundamental absorption band, $\varepsilon = \varepsilon_1 + i\varepsilon_2$ is a complex quantity, whose imaginary part, ε_2 , is determined by the band structure according to the expression [32]:

$$\varepsilon_2(\hbar\omega) = \frac{\hbar^2 e^2}{3\pi m^2 \hbar^2 \omega^2} \sum_{i,j} \int_{E_{ij}=\hbar\omega} |M_{ij}(\vec{k})|^2 \frac{dS}{|\nabla_k E_{ij}(\vec{k})|}, \quad (6)$$

where m is the electron effective mass, dS is an element of an energy surface, M_{ij} denotes the matrix element of the transition between states i and j , and E_{ij} is the energy difference between these states.

The real part, $\varepsilon_1(\hbar\omega)$, is determined through $\varepsilon_2(\hbar\omega)$ by means of Kramers-Kronig relation [32]:

$$\varepsilon_1(\omega) = 1 + \frac{2}{\pi} \int_0^\infty \frac{\omega' \varepsilon_2(\omega')}{\omega'^2 - \omega^2} d\omega'. \quad (7)$$

Fig. 5 shows the spectral dependences $\varepsilon_1(\hbar\omega)$ and $\varepsilon_2(\hbar\omega)$ for sputtered bismuth oxide films whose thickness ranges between 0.07 and $1.34 \mu\text{m}$. It is relevant to first mention that the slow decrease registered on both curves at increasing photon energies is characteristic to the films showing low levels of crystallization. However, two pronounced thresholds, A ($\hbar\omega_1 \approx 4.20 \text{ eV}$) and B ($\hbar\omega_2 = 4.80 \text{ eV}$), can be evidenced on the $\varepsilon_2(\hbar\omega)$ contour, for a film thickness $d \approx 0.07 \mu\text{m}$ (curve 4). An analogous structure is registered in the case of $\varepsilon_1(\hbar\omega)$ spectrum (curve 1). At increased film thickness up to about $0.60 \mu\text{m}$ (curve 5), these particularities maintain, besides two new maximums, C ($\hbar\omega_3 \approx 5.52 \text{ eV}$) and D ($\hbar\omega_4 = 6.15 \text{ eV}$) are evidenced. For further increase of film thickness up to $\sim 1.30 \mu\text{m}$ (curve 6), the general tendency of spectral dependences $\varepsilon_1(\hbar\omega)$ and $\varepsilon_2(\hbar\omega)$ maintains, besides $\varepsilon_2(\hbar\omega)$ spectrum contains the particularities A, B and A*, located in the same spectral range like that of thinner films (curves 4 and 5).

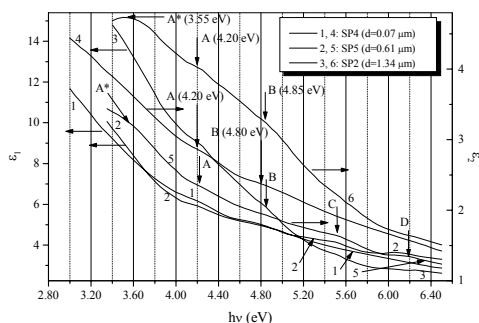


Fig. 5. Optical functions $\varepsilon_1(\hbar\omega)$ and $\varepsilon_2(\hbar\omega)$ of sputtered films.

Consequently, one can state that as-prepared sputtered films are preponderantly amorphous. At the same time, the presence of weak maximums on the ε_2 spectrum certifies the formation of crystallization germs belonging to Bi_2O_3 nanocrystalline incipient phase.

4. Conclusions

In the vicinity of fundamental absorption edge, the optical absorption of sputtered bismuth oxide films is characterized by an optical gap, $E_{\text{ga}}=2.68\text{--}2.73$ eV. The nanocrystalline phase shows a direct optical gap $E_{\text{go}}=3.55$ eV.

The spectral dependences of the optical functions n , k , ε_1 , and ε_2 are determined by prevailing amorphous bismuth oxide phase; besides, the particularities evidenced at about 3.60 eV, 4.30 eV, 4.80 eV, 5.55 eV, and 6.20 eV are due to direct optical transitions between electronic bands formed by bismuth oxide nanocrystallites, whose growth is just initiated.

Acknowledgements

The author would like to thank Dr. A. Visinoiu, for film deposition, and Prof. M. Caraman and Prof. G.I. Rusu for fruitful discussions. He is grateful to Dr. L. Craus for kind assistance in XRD analyses, and Mr. C. Podaru, for AFM scans.

References

- [1] P. Shuk, H.-D. Wiemhöfer, U. Guth, W. Göpel, M. Greenblatt, *Solid State Ionics* **89**, 179 (1996).
- [2] J. George, B. Pradeep, K. S. Joseph, *Phys. Stat. Sol. (a)*, **100**, 513 (1987); *Phys. Stat. Sol. (a)*, **108**, 607 (1987).
- [3] H. Gobrecht, S. Seeck, H.-E. Bergt, A. Märtens, K. Kossmann, *Phys. Stat. Sol.* **33**, 599 (1969); **34**, 569 (1969).
- [4] V. Dolocan, F. Iova, *Phys. Stat. Sol. A* **64**, 755 (1981); V. Dolocan, *Appl. Phys.* **16**, 405 (1978).
- [5] P. B. Clapham, *Br. J. Appl. Phys.* **18**, 363 (1967).
- [6] T. S. Nikolov, M. Aroyo, E. Klein, K. Ikonopisov, *Thin Solid Films* **30**, 37 (1975).
- [7] L. Leontie, M. Caraman, G. I. Rusu, *J. Optoelectron. Adv. Mater.* **2**(4), 385 (2000).
- [8] L. Leontie, M. Caraman, M. Delibas, G. I. Rusu, *Mat. Res. Bull.* **36**, 1629 (2001).
- [9] L. Leontie, M. Caraman, M. Alexe, C. Harnagea, *Surf. Sci.* **507–510**, 480 (2002).
- [10] K. L. Chopra, G. A. Das, *Thin Film Solar Cells*, Plenum Press, New-York-London (1983).
- [11] G. Bandoli, D. Barecca, E. Brescacin, G. A. Rizzi, E. Tondello, *Chem. Vap. Depos.* **2/9**, 238 (1996).
- [12] E. P. Golis, *Proc. SPIE The Int. Soc. Opt. Eng.* **4239**, 2000, p. 23.
- [13] B. L. Yu, A. B. Bykov, T. Qiu, P. P. Ho, R. R. Alfano, N. Borrelli, *Opt. Commun.* **215** (4-6), 407 (2003).
- [14] K. Kikuchi, K. Taira, *Electron. Lett.* **38** (4), 166 (2002).
- [15] R. Balda, J. Fernandez, M. Sanz, A. de Pablos, J. M. Fdez-Navarro, J. Mugnier, *Phys. Rev. B.*, **61** (5), 3384 (2000).
- [16] Z. Shaowu, C. Jigui, L. Yan, L. Xinggin, M. Guangyao, *Sol. State Ionics, Diff.-React.*, **156** (1-2), 197 (2003).
- [17] A. V. Virkar, S. Pomin, Z. F. Kuan, *Metallurg. Mater. Trans. A-Phys. Metall. Mater. Sci.* **33A**(8), 2433 (2002).
- [18] Y. Haixue, L. Chengen, Z. Jiaguang, Z. Weimin, H. Lianxin, S. Yuxin, Y. Youhua, *Mater. Sci. Eng. B-Sol. State, Mater. Adv. Technol.* **B88** (1), 62 (2002).
- [19] A. A. Tomchenko, *Sensors & Actuators B-Chem.* **68** (1-3), 48 (2000).
- [20] T. Hyodo, E. Kanazawa, Y. Takao, Y. Shimizu, M. Egashira, *Electrochem.*, **68** (1), 24 (2000).
- [21] P. Zhou, G. J. You, Y. G. Li, T. Han, J. Li, S. Y. Wang, L. Y. Chen, Y. Liu, S. X. Qian, *Appl. Phys. Lett.* **83** (19), 3876 (2003).
- [22] A. B. Kuz'menko, E. A. Tishchenko, A. S. Krechetov, *Optics & Spectr.* **84**(3), 402 (1998).
- [23] B. Yu, C. Zhu, F. Gan, *J. Appl. Phys.* **82** (9), 4532 (1997).
- [24] D. Chen, Y. Miura, T. Nanba, Y. Murata, A. Osaka, *J. Soc. Mater. Sci. Jpn.* **45/6**, 630 (1996).
- [25] F. H. Pollak, in: *Handbook on Semiconductors, Optical Properties of Semiconductors*, Eds. T. S. Moss and M. Balkanski, North-Holland, Elsevier, Amsterdam, p. 527 (1994).
- [26] E. D. Palik (Ed), *Handbook of Optical Constants of Solids*, Academic Press, New York (1985).
- [27] L. L. Kazmerski (Ed), *Polycrystalline and Amorphous Thin Films and Devices*, Academic Press, N Y (1980).
- [28] J. Tauc, *Optical Properties of Solids*, North-Holland Publ., Amsterdam, p. 277 (1973).
- [29] W. J. Plieth, K. Naegel, *Surf. Sci.* **50**, 53 (1975).
- [30] T. S. Moss, G. J. Burrell, B. Ellis, *Semiconductor Opto-Electronics*, Butterworth Co (Publishers) Ltd., London (1973).
- [31] D. L. Greenaway, G. Harbeke, *Optical Properties and Band Structure of Semiconductors*, Pergamon Press, Oxford (1968).
- [32] M. Cardona, *Solid State Physics, Suppl.* **11**, Modulation Spectroscopy (eds. F. Seitz, D. Turnbull, and H. Ehrenreich), Academic Press, New York and London, p. 25 (1969).

* Corresponding author: lleontie@uaic.ro